

# A SHOCK AMPLIFIER EVALUATION

By: Anthony S. Chu  
Endevco Corporation, San Juan Capistrano, CA 92675

TP293

Anthony Chu, Process Engineering Manager, is responsible for new product development at Endevco Corporation. He has been with Endevco for more than nine years, his areas of expertise include shock transducer design, manufacturing processes, and shock data analysis. Mr. Chu received his Mechanical Engineering degree from California State Polytechnic University, Pomona in 1980, he is current working on his MBA degree at Pepperdine University. Anthony has published several papers in various technical societies, and he has been very active in the field of shock measurement and instrumentation. He is currently an active member of IES Pyroshock Committee, and a member of ISA.

## I. INTRODUCTION

The state-of-the-art of high-g shock measurement has been advancing at a very fast pace during the past few years. There are new products and technologies on the market today that hold great promise in solving our problems in pyroshock measurement. But before these new devices and technologies earn their general acceptance and approval, we must continue to improve our understanding of present system.

Among all the shock and vibration measurement instrumentations, piezoelectric accelerometer and charge amplifier are by far the most commonly used measuring devices in the industry. While accelerometer design has evolved over the years, the basic technology of the charge converter has remained mostly unchanged. Since a high percentage of test labs in the country today still rely on piezoelectric accelerometers as their primary measuring transducer, it is imperative for those users to truly understand the performance of their charge amplifiers before any test data can be accepted confidently.

Back in 1986, Dan Powers of McDonnell Douglas Astronautics Company had performed a charge amplifier evaluations based on a series of pyroshock data taken from a 4' x 8' steel plate. The result of this investigation showed that, although all the amplifiers under test agreed with their claimed specifications and electrical characteristics, each produced markedly different results (SRS) from similar inputs under a controlled shock environment.[1] Upon request from Dan and others, the author has since conducted a more in-depth evaluation of the same amplifier models based on an important assumption which will be stated in the following paragraph.

## II. AN IMPORTANT ASSUMPTION

It has been demonstrated repeatedly that the source of high-g shock excitation (pyro or metal-to-metal impact) imparts acceleration of very high amplitude and short duration. [2] As a result, any near-field measurement using a conventional transducer without any physical isolation may be seriously affected. [3] Consider a piezoelectric shock accelerometer with a designed resonant frequency at 300kHz, first mode. When one places this accelerometer three inches away from the source in a pyroshock test, the ultra-high frequency inputs from the excitation elicits ringing momentarily in the transducer at its resonant frequency, which generates some corresponding electrical signals down the cable, to the charge amplifier. These ultra-high frequency spikes, in most instances, are completely transparent to the user due to either bandwidth limitation in the tape recorder (80kHz max.) or low sampling rate in the digital scope. It is therefore very difficult to convince the test engineer that he/she might have an overload condition in the charge amplifier.

The effects of these high frequency, high amplitude spikes on the shock amplifier are the prime interest in this evaluation.

## III. TEST OBJECTIVES AND CONDITIONS

The objective of this experiment is to compare several commonly use shock amplifiers to examine their output characteristics under momentary overload. The author obtained three charge amplifiers through McDonnell Douglas, Huntington Beach for this test, and five other devices were obtained in-house.

Instead of analyzing their topologies and studying the circuit designs (which in most cases is impossible), the author approached this evaluation as an end user, and examined the data from that point of view. Also for business ethics reason, all unit identifications shall remain anonymous.

The test conditions are as follows:

1. The input signals to the amplifier must resemble outputs from a resonating piezoelectric accelerometer. The input must also be very repeatable.

2. The focus of our attention should be on the residual overload characteristics of these amplifiers because the "instantaneous" overload characteristic is of no consequence to the user if he/she cannot capture it on the time recording. An arbitrary starting point of the analysis window is set at 20 microseconds after time zero--the beginning of the input signal.

3. All amplifiers are set to a overall gain of 1. (lowest possible gain in the first stage) This gain level is commonly used in most shock measurement set-up.

#### IV. TEST SET-UP

Since it is impossible to produce identical outputs from actual pyro-events, an electronic simulation has been used to provide repeatable high frequency input spikes to the charge amplifiers. A 1000 pF capacitor was placed in series at the amplifier front end to simulate charge input. The test set-up is depicted in Figure 1.

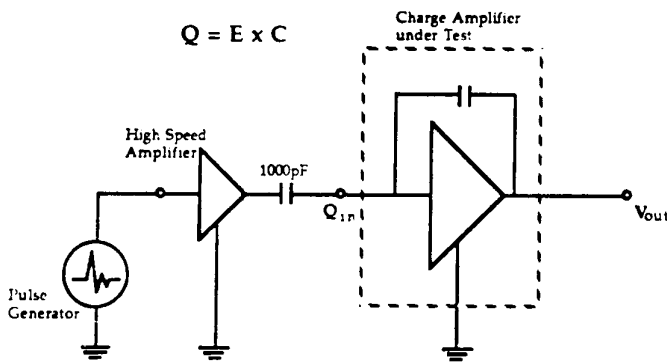


FIGURE 1: Test Set-up, Charge Amplifier Comparison

A programmable waveform generator was used to create the desired pulse shape and duration, and the signal was fed through a high speed power amplifier to get the required voltage swing. Signals were then monitored at both ends of the test amplifier by a digital oscilloscope sampling at 10MHz, 10 bits.

The electronically generated spikes measured at the input end of the test amplifier are shown in Figure 2. This signal resembles the output of a PE accelerometer under pyroshock excitation. The first pulse reaches +40V peak in about 500 nanosecond, and the second

pulse swings immediately to -40V peak. Charge equivalent at this end is 40,000 picocoulomb peak.

There were a total of eight amplifiers in this evaluation. Two from brand X, one from brand Y, and two from brand Z. A general purpose charge amplifier was also included in the evaluation to serve as a baseline for performance. At the end, two hybrid microelectronics amplifiers were added to the agenda to see how they perform under the same condition.

#### V. TEST RESULTS

Before the experiment was conducted, each amplifier was checked against the manufacturer's specification. All units were confirmed to be "normal" within the specified limits. Some critical parameters are listed in Table 1.

	<u>Max. charge input</u>	<u>-3dB point</u>
General Purpose	30,000 pC	29 kHz
X1	50,000 pC	29 kHz
X2	150,000 pC	54 kHz
Y	100,000 pC	178 kHz
Z1	100,000 pC	433 kHz
Z2	30,000 pC	196 kHz
Hybrid	10,000 pC	151 kHz
Hybrid	N/A	150 kHz

TABLE 1: Critical Parameters

It seemed that 40,000 pC was a reasonable input for most of the "shock" amplifiers in this test.

Before we look at the results of these test units, let's define a "good" charge amplifier from the user's perspective. To the test engineer, the amplifier should maintain input signal fidelity within its bandwidth limits, provided that the device has not been driven into saturation. The amplifier should not produce spurious signals or exhibit DC offset when driven by out-of-band input signals. This is particularly important since these out-of-band input signals are "invisible" to most recording equipment, the engineer will never be aware of their presence.

Figure 3 shows the output of the general purpose charge amplifier after being exposed to the nasty but realistic input spikes. The device went immediately into saturation after the event and stayed locked-up at the negative rail. Overload characteristics like this poses no harm to our data analysis because the phenomenon can be readily recognized, and the data will be discarded. After all, a general purpose charge amplifier should not be used in a shock measurement.

Figure 4 shows the output of X1, a widely used charge amplifier in many test labs for shock and vibration measurement. After the input spikes, X1 also went into saturation and stayed at its positive rail (+7V). This characteristic again is immediately recognizable upon playback, and the data will be discarded. Since the maximum input rating of this amplifier was only 50,000 pC, the input was then reduced to 20V peak (20,000 pC) for a second test. Figure 5 shows the response of the device at the reduced input level. A minor but noticeable lower frequency signal was produced as a result of the input spikes. This signal is purely a by-product of the amplifier's idiosyncrasy which can cause distortions in subsequent data reduction. Due to its low amplitude (40 mV) and the masking effect of the real signals, these spurious characteristics will not catch the attention of the test engineer and analyst.

Figure 6 shows the output of X2 with the original (40 Vp) input spikes. At first glance, this amplifier had only modified (filtered?) the shape of the bidirectional input spikes and produced a unidirectional pulse of 10  $\mu$ S in duration. For most recording devices, the pulse is invisible, so one may conclude that this is an acceptable amplifier. But when the vertical resolution on the digital scope was expanded (see Figure 7), however, a -80mV zershift was noticed. Again this minor DC offset can be completely undetectable to the naked eyes, but its effect at the low end of the Shock Response Spectrum is tremendous. Consider that X2 is one of the most widely used shock amplifiers in the field, the implication is far reaching.

Figure 8 shows the response of Y, also a commonly used charge amplifier. This device produced two unrelated peaks after it was exposed to the input spikes. But the durations are so short that they probably will not get into the data recording, and therefore poses no harm. Expanding the vertical resolution (not shown here) showed no sign of DC offset, making it an acceptable charge amplifier for pyroshock application.

Figure 9 shows the output of Z1. This amplifier produced an output closely resembling the input spikes. Expanding the resolution on the digital scope shows no sign of zershift (see Figure 10). This amplifier would be a safe choice for near-field shock applications.

Figure 11 shows the response of Z2, a more modest device from the point of view of claimed performance. This amplifier went immediately into saturation after the input had struck, but it recovered almost instantaneously and returned to "zero" in less than 15  $\mu$ S. Close examination of the output also showed no sign of DC offset. This amplifier can also be considered for near-field shock measurement.

Figures 12 and 13 show the outputs of the hybrid microelectric circuits. Both circuits reacted to the input spikes and recovered instantly without exhibiting any secondary effect after 20  $\mu$ S. These amplifiers are currently used in several shock accelerometers with internal signal conditioning.

Up to this point, all the amplifiers were tested in their broadband configuration. Many practitioners of pyroshock measurement, however, use low-pass filter in their daily work. Since two of the test units have built-in filtering features conveniently located on the front panel, additional tests were run to see how these filters behave under the same input condition. (The author did not evaluate any external input low-pass filters due to the limited scope of this paper)

Figure 14 shows the response of Y, with a 10 kHz 2-pole low-pass filter switched in. It is curious to notice a big hump (+0.7 V, lasting 80  $\mu$ S) right after the impulse response. When one calculates the spectrum of this time history to 10 kHz, the energy in this hump will certainly appear in the data. Figure 15 shows a similar response of Y when the filter was set at 3 kHz. Only this time the hump got smaller, and the duration was much longer.

Figure 16 shows the filtered (5 kHz) output of Z1. Z1, with the low-pass filter in the circuit, seems to suppress the input spikes effectively, but a positive hump (+0.9 V, lasting 50  $\mu$ S) is still present. Its energy, however, will only appear in the spectrum above 10 kHz.

To help the author understand this interesting filter behavior, a computer simulation was performed by modeling a one-sided 5  $\mu$ S pulse into a "perfect" 2-pole Butterworth low-pass filter. The output is shown on Figure 17 in which a similar hump is also evident. It is obvious that the phenomena observed in our test have not been caused by saturation, but rather are a natural response of the filter to a near-impulse input. The implications of this finding should trigger some re-thinking of applying low-pass filter in shock measurement, and this subject certainly warrants further investigation.

## VI. CONCLUSIONS

Is there any correlation between amplifier performance and claimed specification? Table 2 summarizes the test results:

	<u>DC Offset</u>	<u>Max. input</u>	<u>-3dB point</u>
General Purpose	>10V	30,000 pC	29 kHz
X1	>7V	50,000 pC	29 kHz
X2	80mV	150,000 pC	54 kHz
Y	0	100,000 pC	178 kHz
Z1	0	100,000 pC	433 kHz
Z2	0	30,000 pC	196 kHz
Hybrid	0	10,000 pC	151 kHz
Hybrid	0	N/A	150 kHz

TABLE 2: Test Summary

Two observations can be made here. First, a high "maximum charge input" rating does not alone qualify a unit as a good shock amplifier. Secondly, wide bandwidth seems to correlate well with good overload characteristics. From this amplifier evaluation the author concluded that, in the presence of high amplitude, fast rise-time transient inputs as found in near-field shock measurement, three out of the six test amplifiers exhibited DC offset after the transient response. While an obvious DC offset may be detected easily by the test engineers, the minor zero shifts may be left unchecked and cause serious low frequency errors in Shock Response Spectrum calculations.

The charge amplifiers from both brand Y and Z in our test can be recommended for shock application. There are however many more shock amplifiers on the market than the author has included in this evaluation. It is therefore important for the end users to verify their performance before using. Both of the hybrid microelectronic circuits exhibited acceptable overload recovery characteristics and did not generate any undesirable secondary effects.

Our findings of the low-pass filter experiment re-

minds us once again that a true impulse contains broadband energy. Our result has shown that, when feeding a low-pass filter with near-impulse signals, a characteristic hump was created at the output which represents the low frequency energy content of the impulse. These "low frequency" components are real, and they are just part of the input.

## VII. REFERENCES

1. A. E. Galef, "The Pre-Pulse in Pyroshock Measurement and Analysis", Bulletin, 56th Shock & Vibration Symposium, Part III, 1986.
2. D. Powers, "Pyroshock Instrumentation", Paper presented at the SAE G-5 Committee Meeting, October 6, 1988.
3. A. Chu, "A Shock Accelerometer with Built-in Mechanical Filter", Bulletin, 59th Shock & Vibration Symposium, Part I, 1988. Sandia Report SAND88-2473C.

# Input Spikes

REPORT # BI-DIRECTIONAL

DATE: 10-20-89

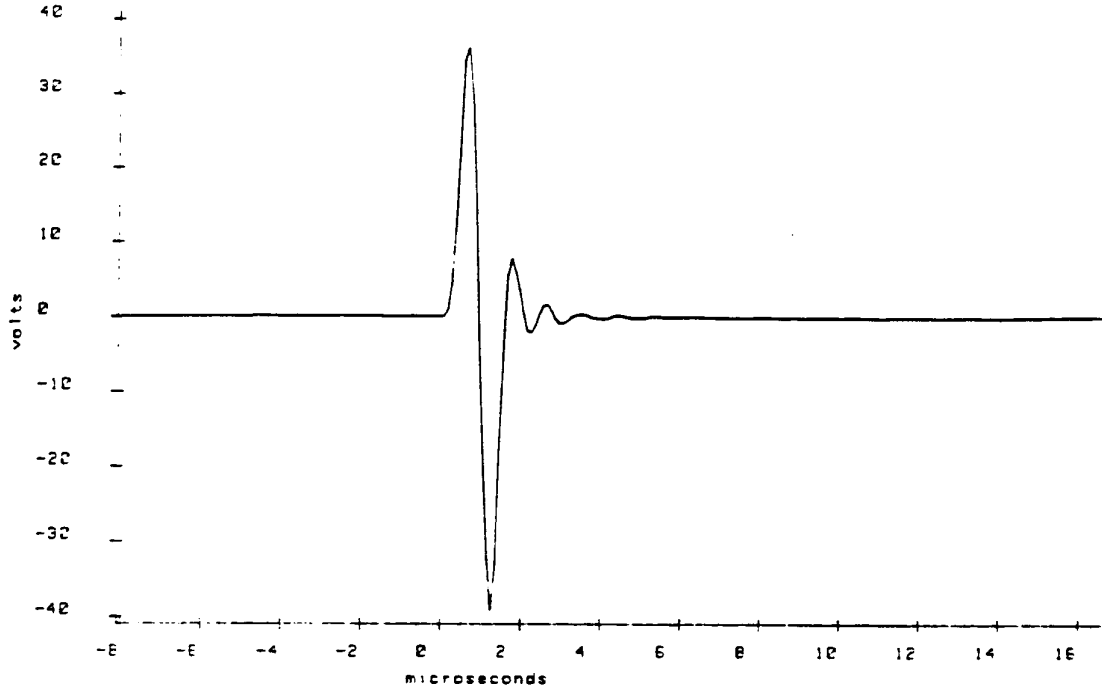


FIGURE 2

# General Purpose Charge Amplifier

REPORT # BI-DIRECTIONAL

DATE: 10-20-89

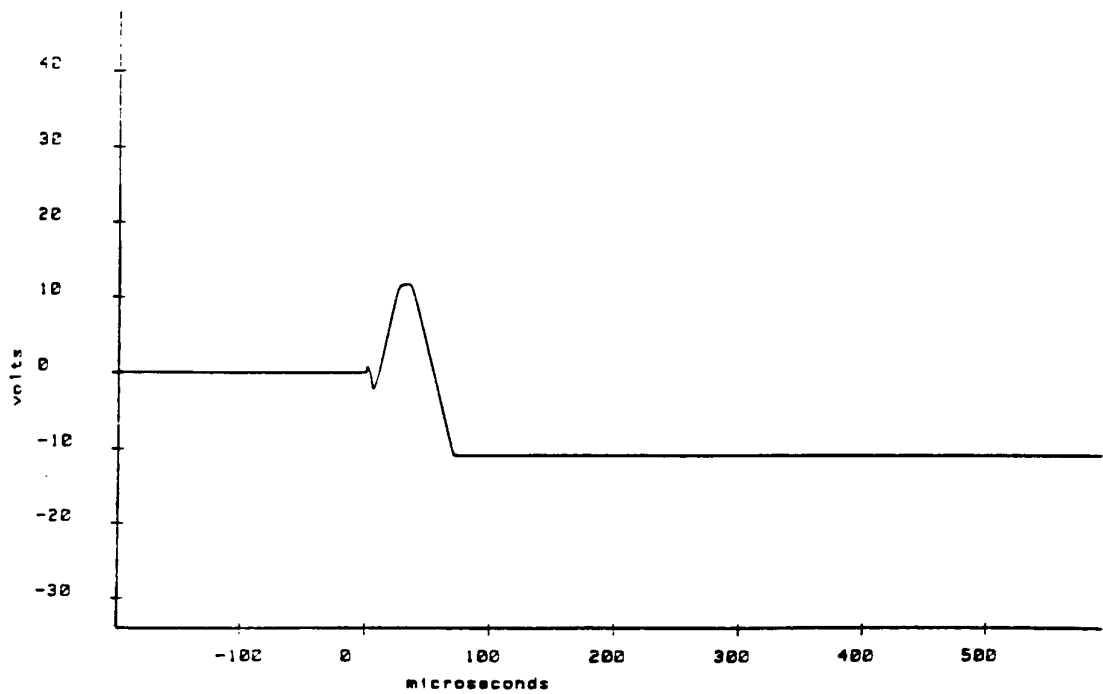


FIGURE 3

MODEL ♦ X1  
SERIAL ♦ N/A

REPORT ♦ BI-DIRECTIONAL  
DATE: 10-20-89

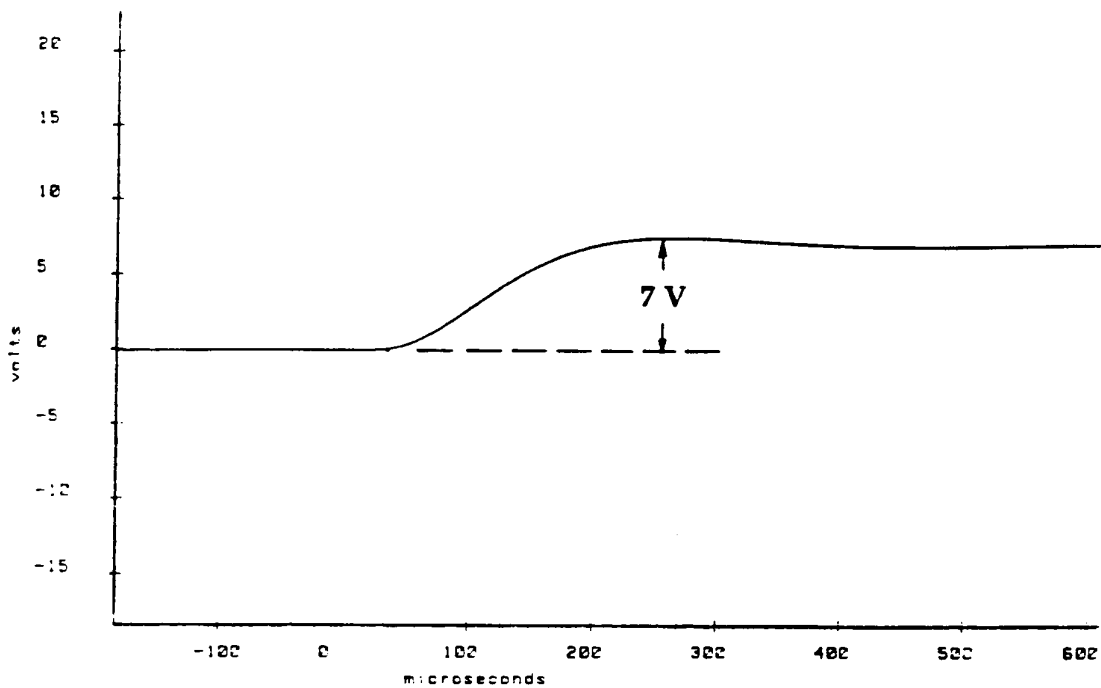


FIGURE 4

MODEL ♦ X1  
SERIAL ♦ N/A

REPORT ♦ BI-DIRECTIONAL  
DATE: 10-20-89

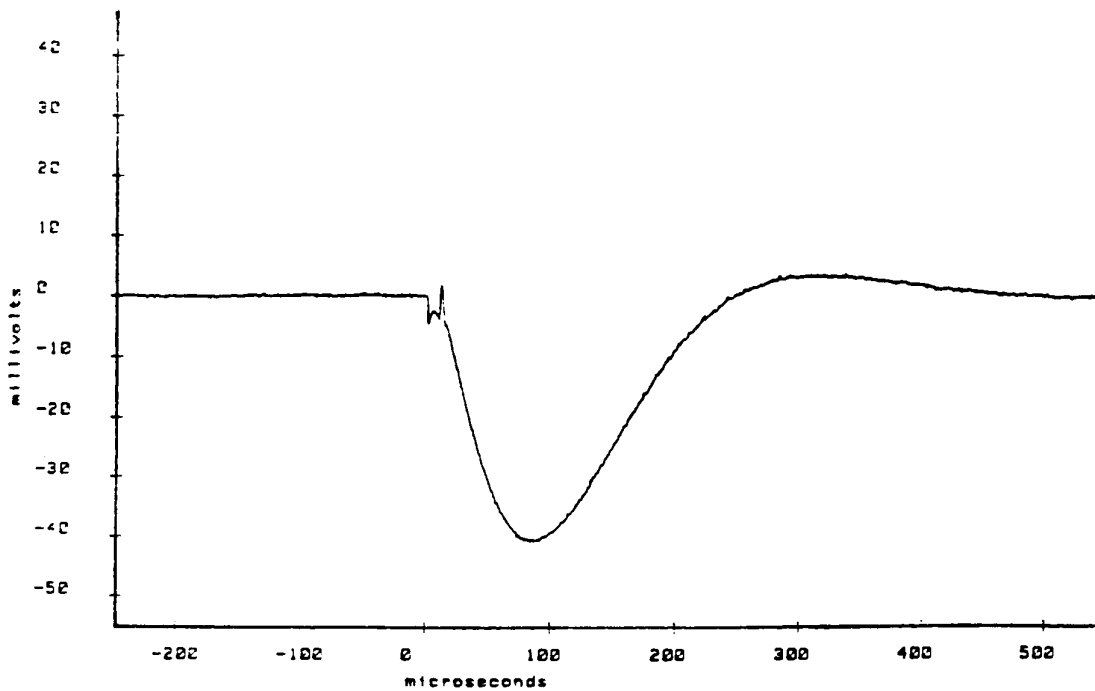


FIGURE 5

MODEL ♦ X2  
SERIAL ♦ N/A

REPORT ♦ BI-DIRECTIONAL  
DATE: 10-20-89

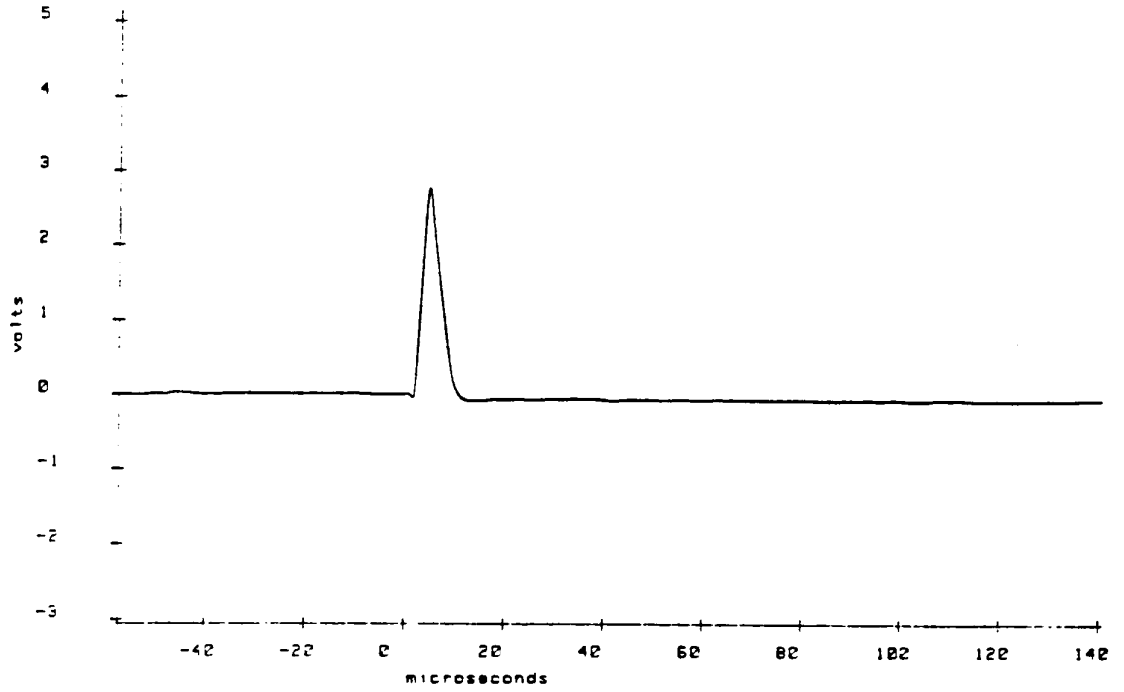


FIGURE 6

MODEL ♦ X2  
SERIAL ♦ N/A

REPORT ♦ BI-DIRECTIONAL  
DATE: 10-20-89

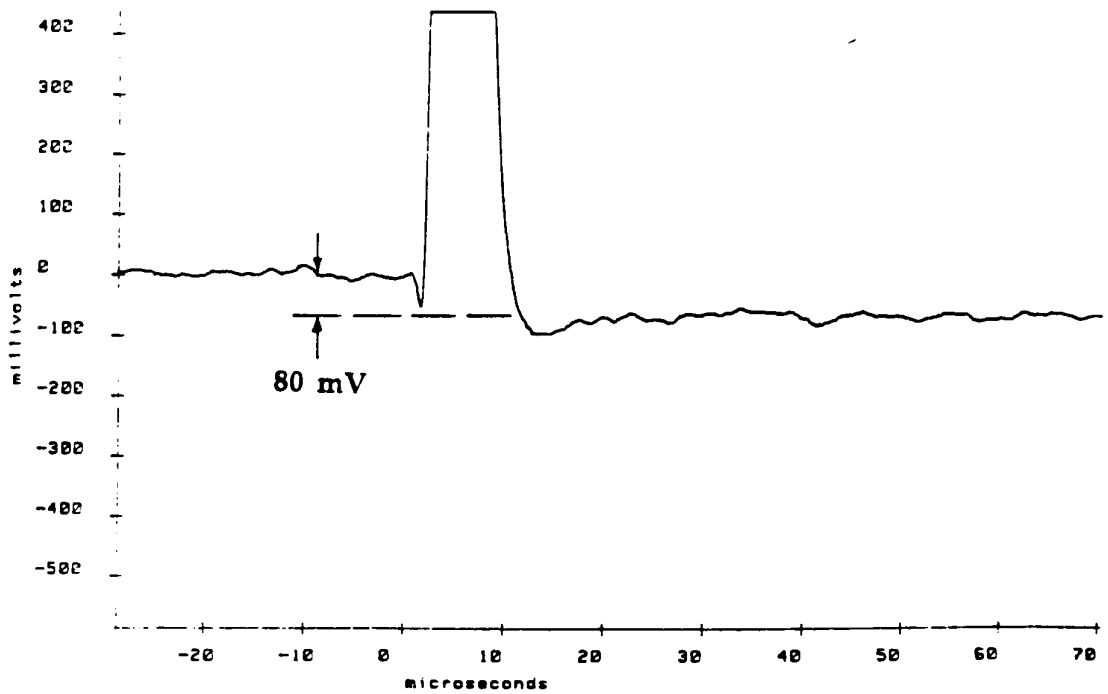


FIGURE 7

MODEL \* Y  
SERIAL \* N/A

REPORT \* BI-DIRECTIONAL  
DATE: 10-20-89

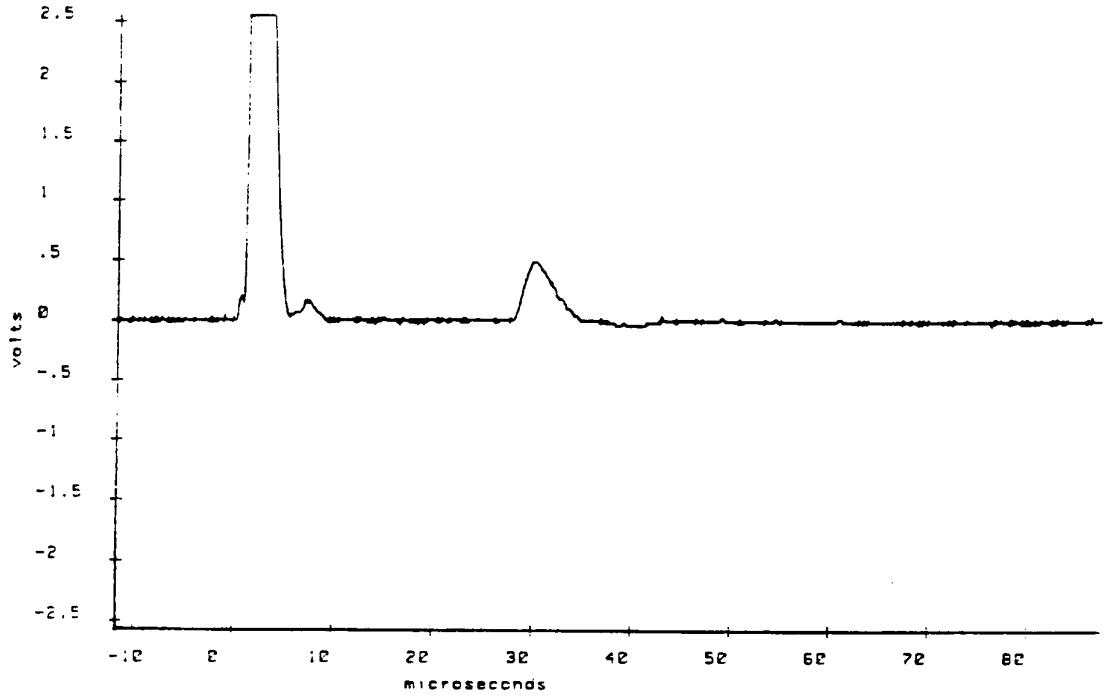


FIGURE 8

MODEL \* Z1  
SERIAL \* N/A

REPORT \* BI-DIRECTIONAL  
DATE: 10-20-89

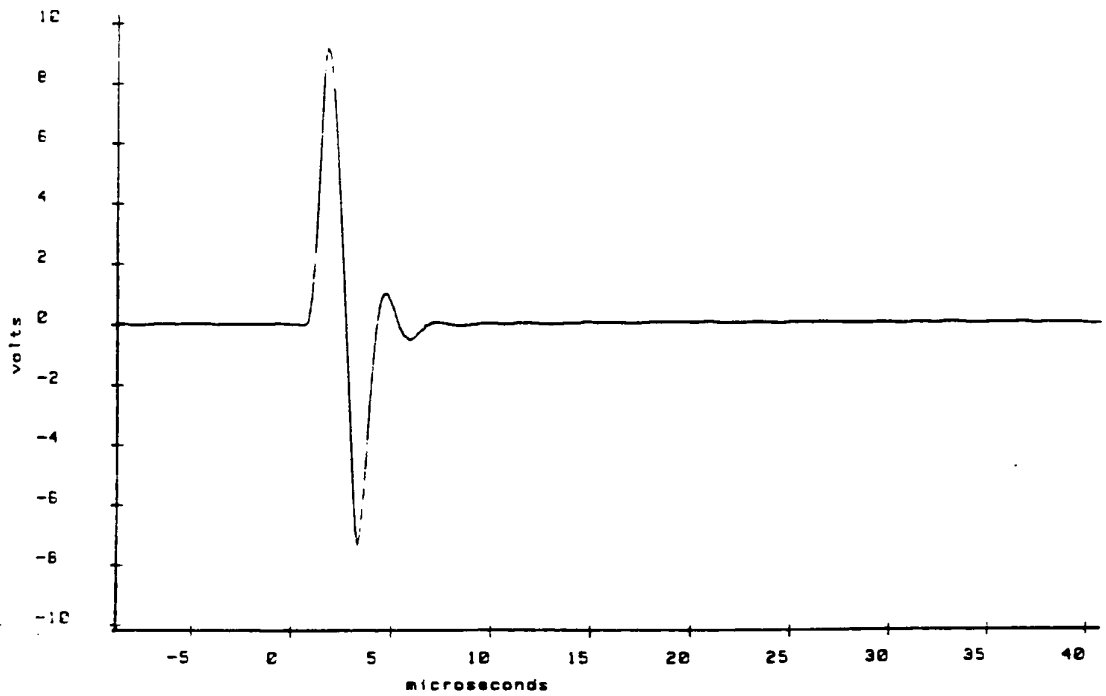


FIGURE 9

MODEL ♦ Z1  
SERIAL ♦ N/A

REPORT ♦ BI-DIRECTIONAL  
DATE: 10-20-89

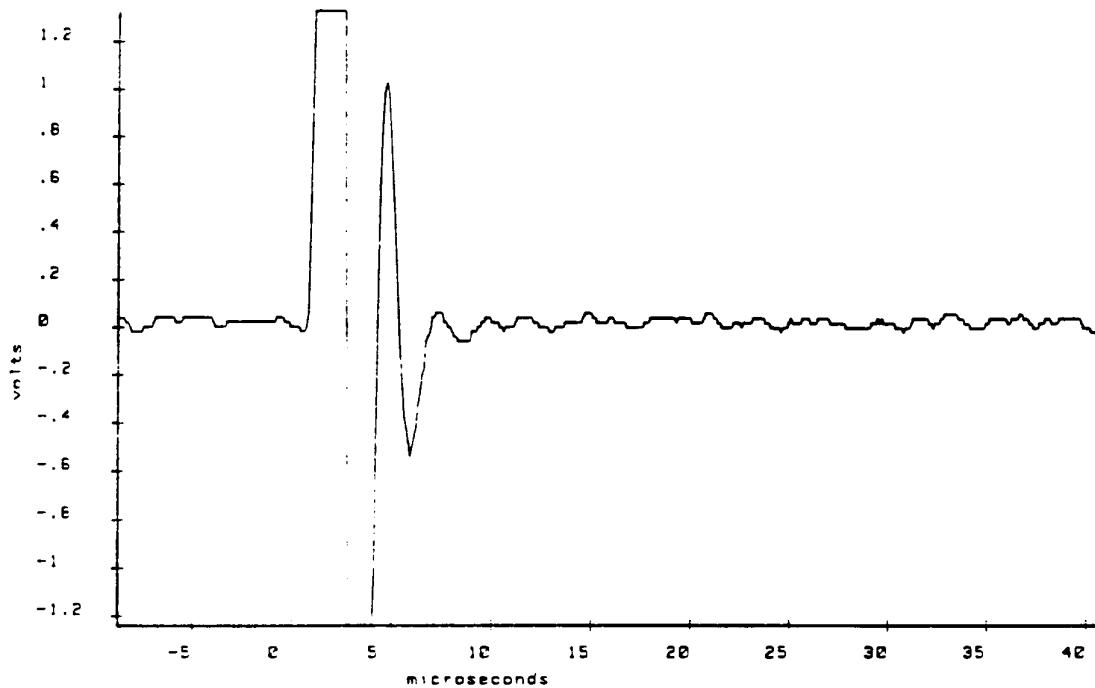


FIGURE 10

MODEL ♦ Z2  
SERIAL ♦ N/A

REPORT ♦ BI-DIRECTIONAL  
DATE: 10-20-89

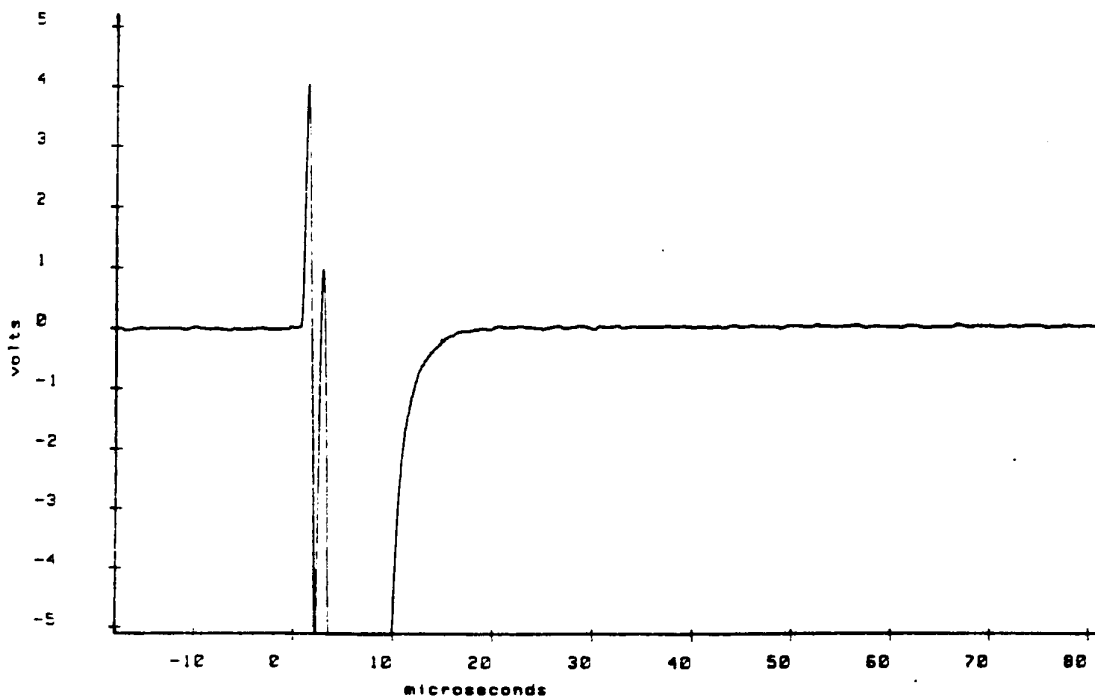


FIGURE 11

# Hybrid Charge Convertor

REPORT ♦ BI-DIRECTIONAL

DATE: 10-20-89

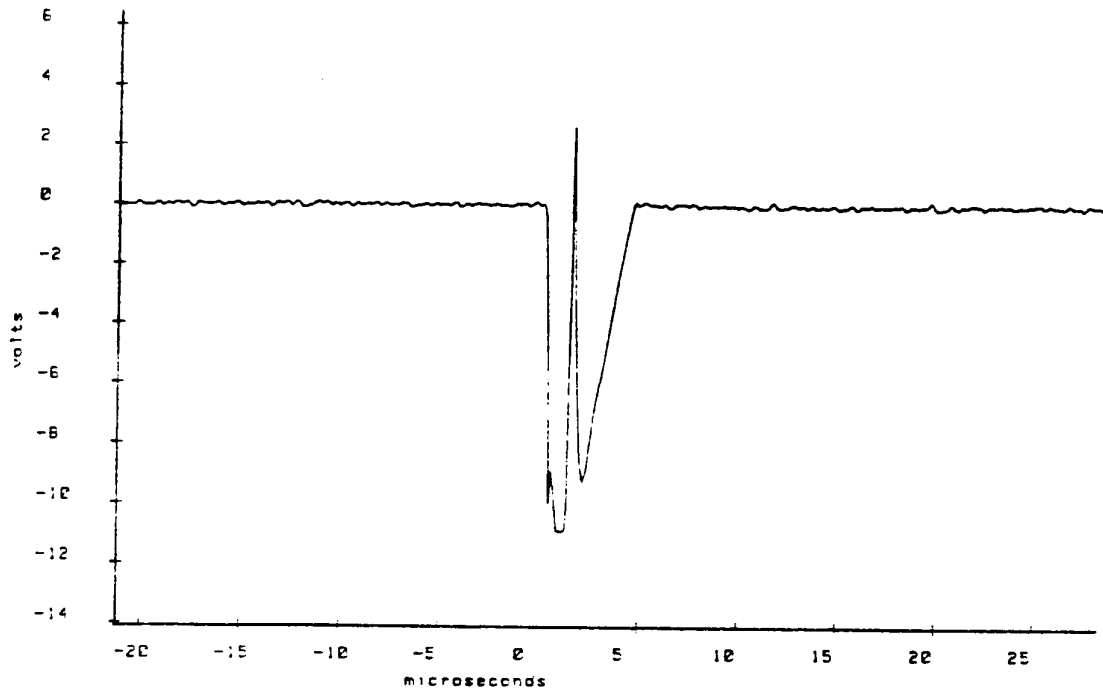


FIGURE 12

# Hybrid Voltage Follower

REPORT ♦ BI-DIRECTIONAL

DATE: 10-20-89

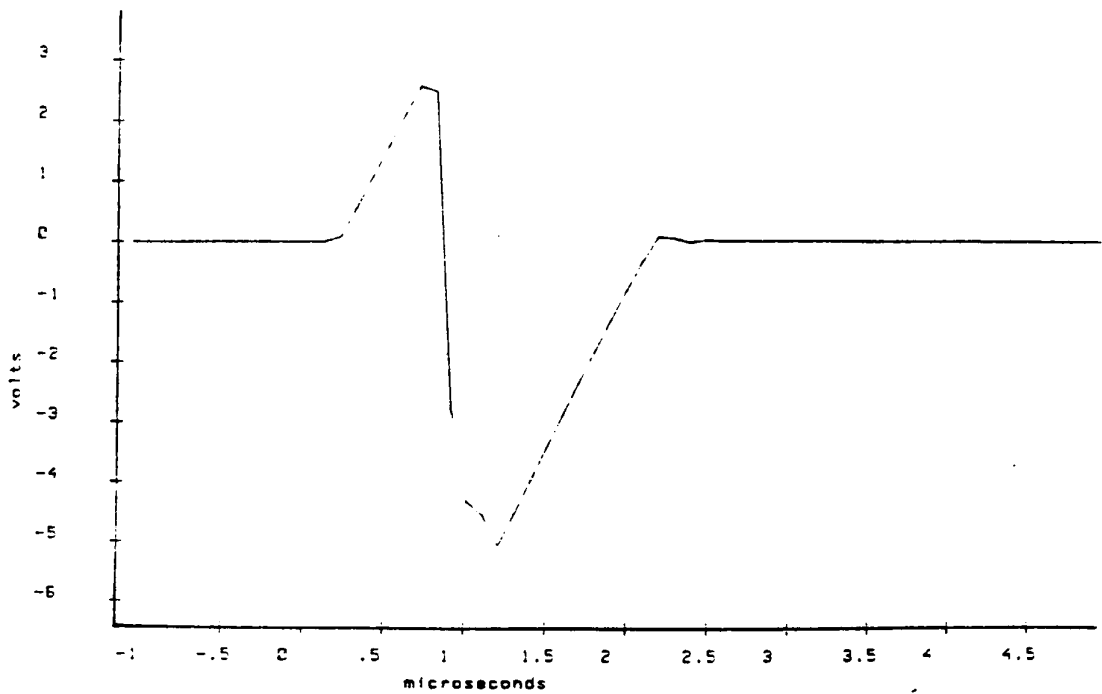


FIGURE 13

MODEL ♦ Y 10KHZ LP  
SERIAL ♦ N/A

REPORT ♦ BI-DIRECTIONAL  
DATE: 10-20-89

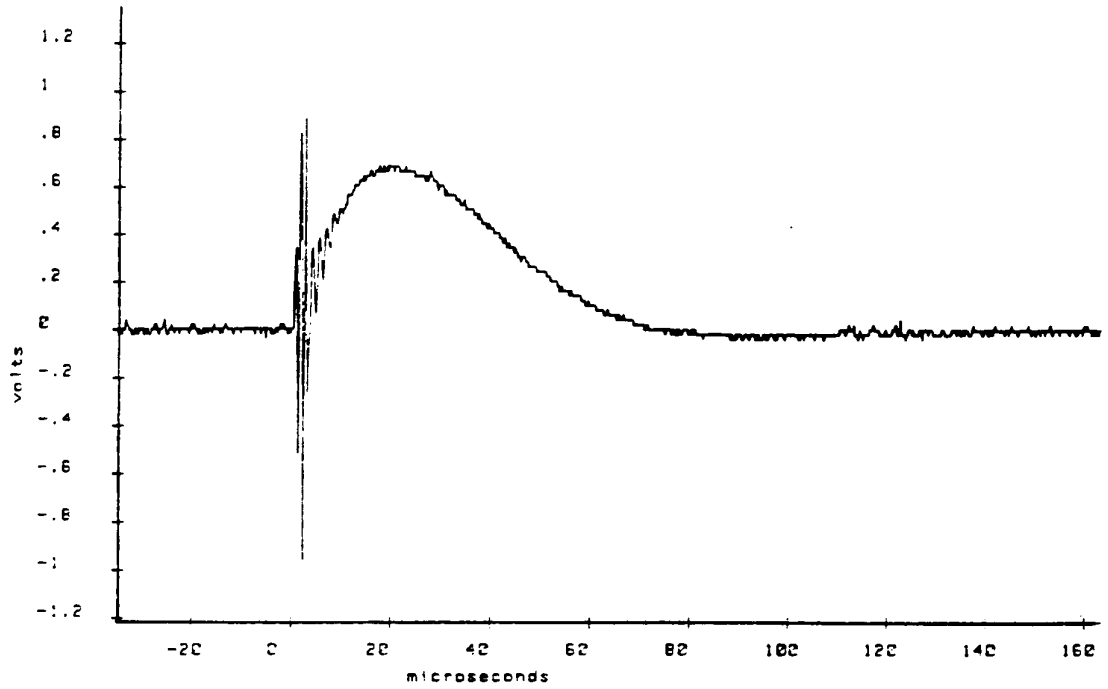


FIGURE 14

MODEL ♦ Y 3KHZ LP  
SERIAL ♦ N/A

REPORT ♦ BI-DIRECTIONAL  
DATE: 10-20-89

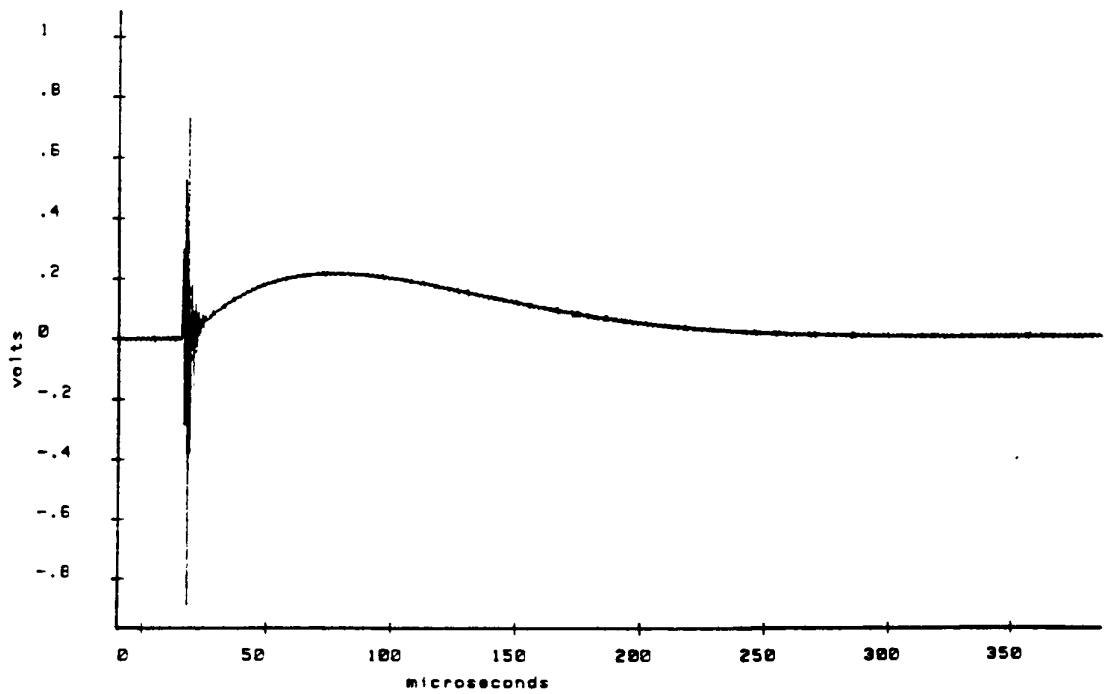


FIGURE 15

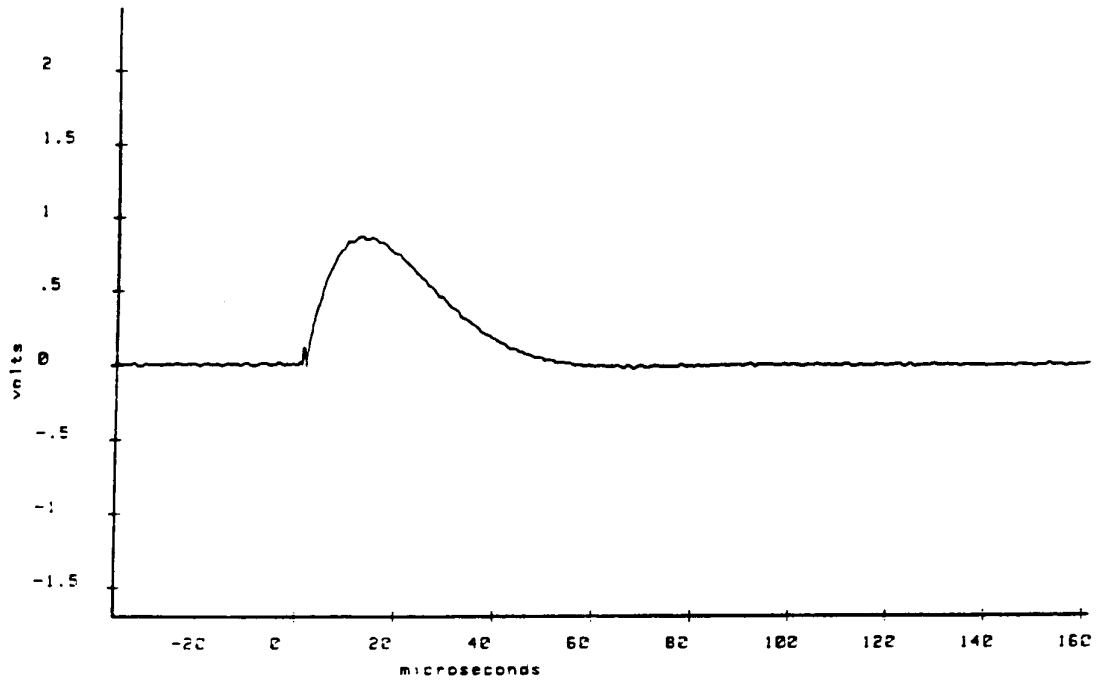


FIGURE 16

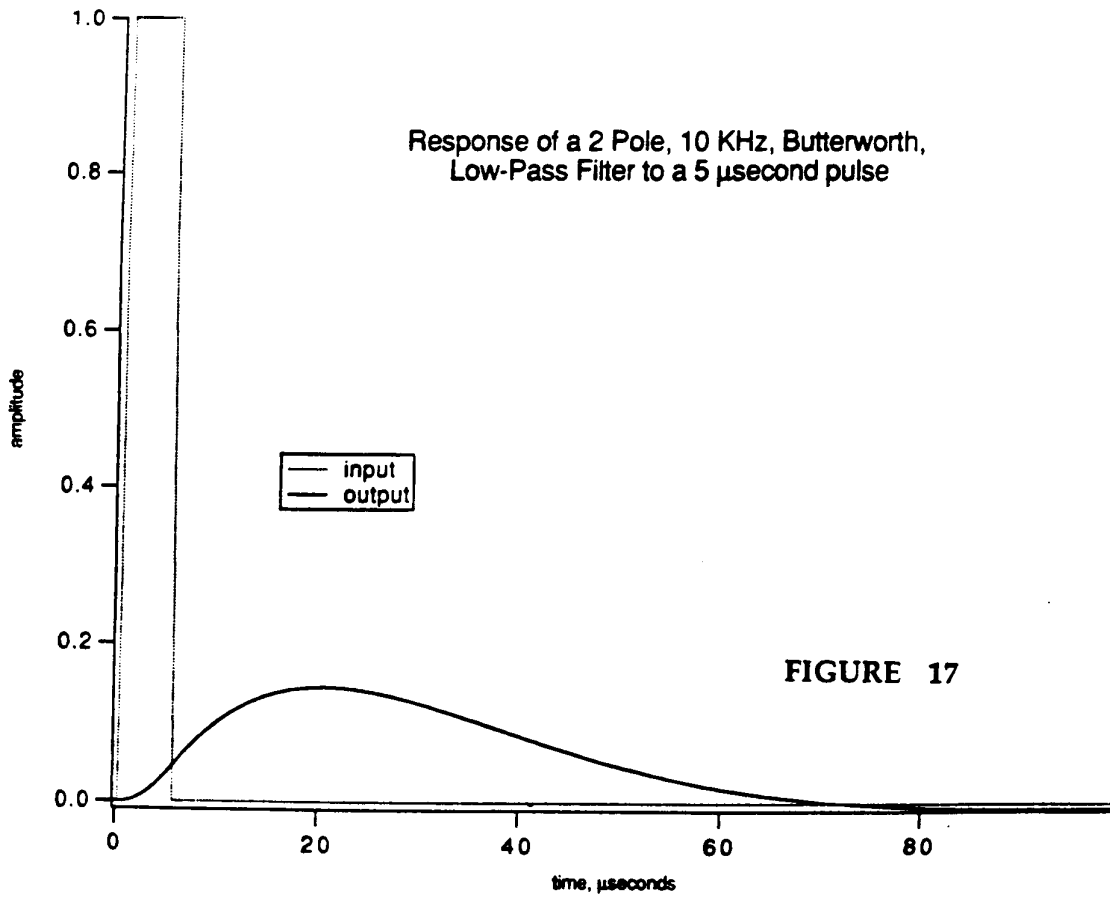


FIGURE 17